Monte Carlo Simulations of a Recent Kinetics Mechanism for the Reduction Reaction of NO by CO on Percolation Clusters

Joaquín Cortés* and Eliana Valencia

Faculty of Physical Science and Mathematics, University of Chile, P.O. Box 2777, Santiago, Chile

Received April 22, 2008; E-mail: jcortes@dqb.uchile.cl

The behavior of a recent kinetics mechanism for the reduction reaction of NO by CO on the surface of a series of percolation clusters is studied by means of Monte Carlo simulations using experimental rate constant values from the literature. The structural sensitivity of the reaction is observed through the production curves and phase diagrams. The kinetics phase transitions and the relation between production and the mean number of nearest neighbors of the cluster's active site, the temperature and the pressure of the gas-phase components are analyzed.

Over the last 30 years kinetics models of surface reactions have attracted the attention of chemists because of their importance in catalysis, and of physicists because they are good examples for the study of irreversible dynamics systems that exhibit complicated behaviors, including dissipative structures, oscillations, kinetics phase transitions, etc.[1] That is the case of the catalytic reduction of NO by CO (CO–NO reaction) on noble metals, which has been studied extensively by experimenters because of its importance in catalytic converters used to control NO_x emissions from mobile sources such as automotive exhaust gases.[2] On the other hand, this reaction has been a classical prototype of nonequilibrium systems, which have been very well reviewed by Evans,[3] Zhdanov and Kasemo,[4] and Albano.[5] With the purpose of interpreting the experimental information on the CO–NO reaction by means of the kinetics mechanism, the literature shows an interesting evolution of a discussion, not devoid of controversy, from the first papers by Hecker and Bell,[6] Oh et al.,[7] and Cho.[8] Later, as a result of experimental work with rhodium, Permana et al.[9] and Peden et al.[10] proposed a Langmuir–Hinshelwood (LH) type mechanism for this reaction that has been largely accepted in current literature. Chuang and Tan,[11] on the other hand, have suggested a new mechanism that takes into account the existence of the positively or negatively charged NO species $Rh–NO^+$ and $Rh–NO^-$ on the surface, which would describe the behavior of the CO–NO reaction on supported Rh catalysts. Research on this mechanism is very recent, however, and the values of its kinetic constants are still unknown.

In recent years, a series of interesting experiments carried out by Zaera's group at the University of California for the CO–NO reaction on Rh using nitrogen isotopes[12] and molecular beam studies,[13] led to a new view of the microscopic behavior of the reaction. In a recent paper by our group,[14] the kinetics mechanism shown in Scheme 1 was proposed, providing a reasonable interpretation of the old results of Permana et al.[9] and the new findings of the experiments of Zaera. This mechanism considers the adsorption stages of CO and NO from the gas phase on site S of the surface and the desorption of the adsorbed molecules $CO_{(a)}$ and $NO_{(a)}$. The $NO_{(a)}$ particles have, beside the possibility of desorption, that of dissociating into the superficial atoms $N_{(a)}$ and $O_{(a)}$ or reacting with $N_{(a)}$ in a stage that produces N_2O and another one that produces N_2, in the latter case leaving an oxygen atom $O_{(a)}$ on the surface. This last stage replaces the beta stage of the LH reaction between adsorbed nitrogen, $N_{(a)}$, for the production of N_2 proposed in previous schemes. Finally, the reaction between $CO_{(a)}$ and $O_{(a)}$ allows the production of CO_2. The rate constants k_i of the (i) stage have been shown in the scheme in each of the cases.

From a basically theoretical standpoint, the CO–NO reaction has been the subject of a number of very interesting papers that include computer simulations and mean field models. The

$CO + S \xrightarrow{k_1} CO_{(a)}$	$NO_{(a)} + S \xrightarrow{k_5} N_{(a)} + O_{(a)}$
$CO_{(a)} \xrightarrow{k_2} CO + S$	$CO_{(a)} + O_{(a)} \xrightarrow{k_6} CO_2 + 2S$
$NO + S \xrightarrow{k_3} NO_{(a)}$	$NO_{(a)} + N_{(a)} \xrightarrow{k_7} N_2O + 2S$
$NO_{(a)} \xrightarrow{k_4} NO + S$	$NO_{(a)} + N_{(a)} \xrightarrow{k_8} N_2 + O_{(a)} + S$

Scheme 1. Mechanism of the CO–NO reaction used in the paper (Ref. 14).

Published on the web October 10, 2008; doi:10.1246/bcsj.81.1267

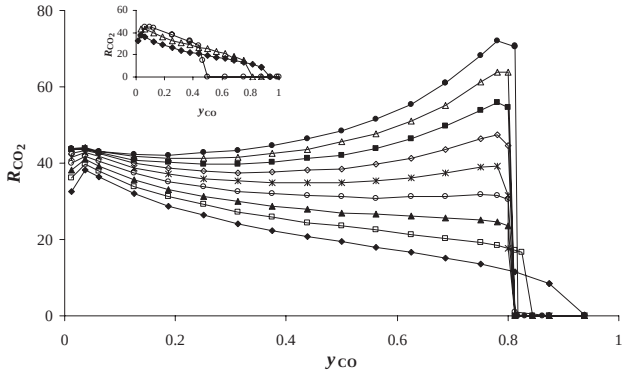

Figure 1. Production (R_{CO_2}, y_{CO}) in the steady state for the mechanism of Scheme 1 obtained from MC simulations on percolation clusters for r equal to: (●) 0.0; (△) 0.05; (■) 0.10; (◇) 0.15; (∗) 0.20; (○) 0.25; (▲) 0.30; (□) 0.35; (◆) 0.407254 (IPC) $T = 623$ K. The lines have been drawn to guide the eyes. The top insert shows the CO production curve in the case of the IPC when the frequency factor ν_i is equal to (◆) 2.1×10^{10}; (△) 2.7×10^{10}; (○) 3.3×10^{10}.

first Monte Carlo simulations made by Yaldram and Khan[15] and Evans et al.[16] made use of a simplified mechanism that led to a poisoned system, a situation that was later explained by Brosilow and Ziff[17] through the checkerboad argument, which our group has recently extended to the study of the surface of a three-dimensional fractal.[18] In some of our recent papers,[14,19] we have carried out some Monte Carlo simulations of this reaction considering the mechanism proposed by Permana et al.[9] and Peden et al.,[10] and the experimental values of the kinetics constants proposed in the literature, with the purpose of commenting some theoretical aspects while keeping the discussion close to the experimental data.

The behavior of the CO–NO reaction has also been discussed by means of the development of a simplified mean field model of its dynamics equations by Evans et al.[16] Later, our group[20] used a pairs approximation and a more complex mechanism that interpreted adequately the Monte Carlo results. Dickman et al.[21] also studied the case of networks with higher coordination numbers.

Permanent interest in this important reaction has led us to introduce in this paper a study of Monte Carlo simulations of the CO–NO reaction, assuming the new mechanism of Scheme 1 on a number of substrates corresponding to percolation clusters from a uniform surface to the incipient percolation cluster (IPC) fractal. This allows the study of the behavior of the surface and the productivity of the process when surface disorder increases in relation to a decreasing coordination number of the active site, which validates, as noted in the literature with respect to these substrates,[5,22] the supported catalysts that are used in the experiment.

Results and Discussion

The kinetic behavior of the CO–NO reaction studied by Monte Carlo simulations is represented first through the production curves of Figure 1 and the phase diagrams of Figure 2 for the series of substrates corresponding to percolation clusters obtained by blocking different proportions r of surface

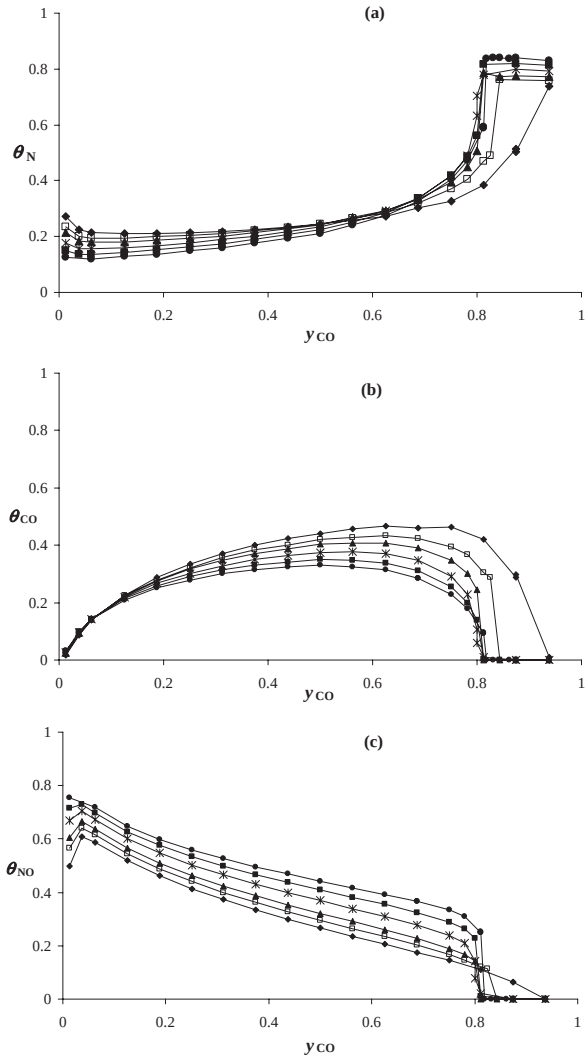

Figure 2. Phase diagram (θ_i, y_{CO}) from MC simulations corresponding to Figure 1. The symbols of the percolation clusters are the same as in Figure 1. (a) $N_{(a)}$. (b) $CO_{(a)}$; (c) $NO_{(a)}$. The lines have been drawn to guide the eyes.

sites. The activity of CO_2 (R_{CO_2}) and the covered fractions of the various species (θ_i) in the phase diagram have been graphed as functions of the fraction of CO in the gas phase, y_{CO}, for a total pressure $P_{CO} + P_{NO}$ equal to 16 Torr.

The most relevant details of MC simulations, are given in Appendix where, among other things, it is explained how the lattice used in the MC simulation is representative of the catalytic surface of the experimental system. The MC moreover assumed the validity of the mechanism of Scheme 1 and used the rate constants shown in Table 1. Those constants, which we have discussed and used in a recent paper,[14] were obtained from the pertinent literature as shown in the table. Constant k_7, on the other hand, was determined from constant k_8 by means of

$$R_{N_2}/R_{N_2O} = k_8/k_7 \quad (1)$$

which was obtained directly from the expressions for the production of N_2 and N_2O. Equation 1 makes it possible to use the data of Permana et al.[9] for the selectivity S_{N_2O} defined by

Table 1. Kinetics Parameters from Rh(111) Used in the Paper[a)]

Event	Activation energy E_i/kJ mol^{-1}	Frequency factor ν_i/s^{-1}	References
CO desorption (k_2)	$132.3 - 18.8\theta_{CO} - 41.9\theta_N$	1.6×10^{14}	7
NO desorption (k_4)	124.4	4.6×10^{14}	23
NO dissociation (k_5)	$73.3 + 8.4\theta_{NO}$	2.1×10^{10}	23
CO_2 production (k_6)	59.9	10^{12}	7
Delta N_2 production (k_8)	87.9	2×10^9	7

a) Selectivity $S_{N_2O} = 0.8$ for $T = 623$ K of Ref. 9.

$$S_{N_2O} = R_{N_2O}/(R_{N_2} + R_{N_2O}) \quad (2)$$

determining k_7 as a function of k_8 from

$$k_7 = k_8 S_{N_2O}/(1 - S_{N_2O}) \quad (3)$$

In this way it is possible to obtain a reasonable value for constant k_7, allowing the conceptual analyses of the systems studied to remain within a range of orders of magnitude close to the experimental data. According to Permana et al.,[9] the selectivity, S_{N_2O}, remains constant at a value of approximately 0.8, with CO and NO pressures in the range of $1 < P_{CO} < 40$ and $1 < P_{NO} < 40$ Torr and temperatures in the range of $500 < T < 700$ K, which were the ranges used in this work, allowing us to keep a constant selectivity in the analyses made.

The chosen selectivity of 0.8 relates the production of N_2O with that of N_2. On the other hand, since the stoichiometry of the reaction allows writing the following relation,

$$R_{CO_2} = 2R_{N_2} + R_{N_2O} \quad (4)$$

only one production value is independent, as in the case of CO_2 production, which has been graphed in Figure 1.

The results of the simulations have a number of interesting aspects. In the first place, a structural sensitivity of the CO–NO reaction is seen, which appears in the production diagrams over the different percolation clusters, from the uniform surface to the IPC fractal, validating the effect of the catalysts' particle size in the real experiment, where a lower production occurs if particle size decreases. This aspect was considered originally by Casties et al.[22] by assuming that the percolation clusters are a good model of some characteristics of catalytics particles of various sizes. These particles show increasing disorder as their size decreases, a situation that is homologated by the model's clusters which, as the value of r increases, decrease their neighbors around the site representing a situation of greater disorder. The activity differences seen in Figure 1 for surfaces of diverse disorder are therefore an indication that the system is structurally sensitive.

Figure 1 also shows in the high CO pressure zone, for the case of a uniform substrate ($r = 0$), a discontinuity corresponding to a first-order irreversible phase transition (IPT) between an active zone and a degenerate sector poisoned with superficial nitrogen and oxygen, a situation that is visualized in the snapshot of Figure 3a, which shows that all the particles of adsorbed oxygen are surrounded by adsorbed nitrogen atoms. Since neither of these particles are desorbed, and the mechanism excludes the beta nitrogen formation stage, the system will remain permanently poisoned. On the other hand, the degeneration of the adsorbent zone makes this transition

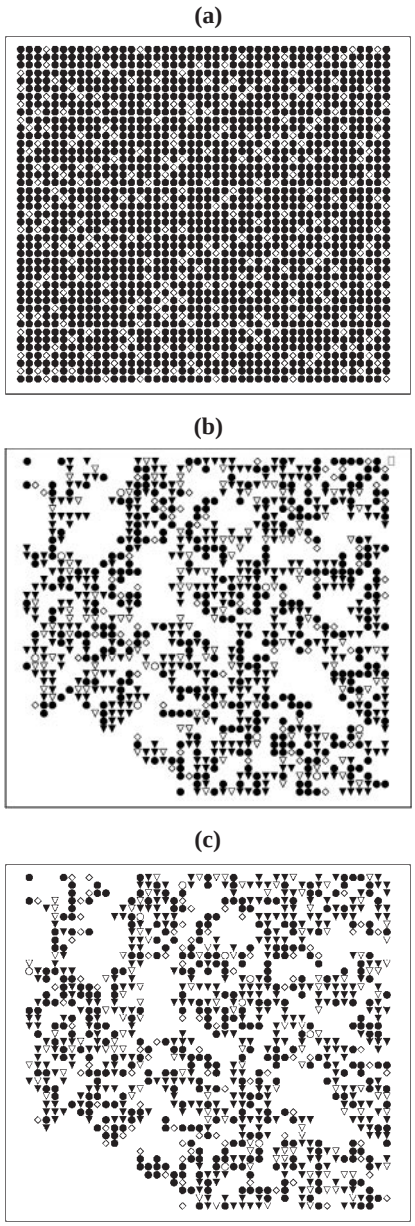

Figure 3. Snapshots of the MC simulations at 623 K corresponding to the diagram of Figure 1; (◇) O; (●) N; (▼) CO; (▽) NO; (○) vacuum. (a) uniform surface, $y_{CO} = 0.875$; (b) IPC 100×10^6 MCS, $y_{CO} = 0.8125$; (c) IPC 500×10^6, $y_{CO} = 0.8125$.

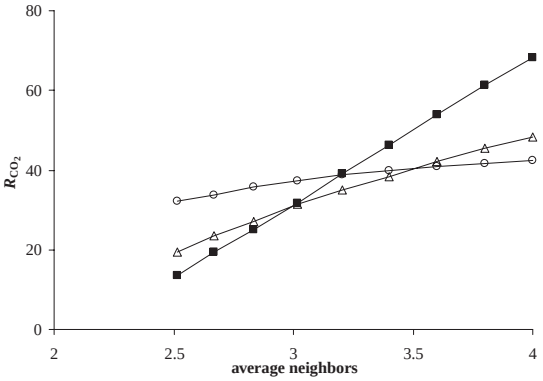

Figure 4. R_{CO_2} production versus the average of the number of nearest neighbors, q_i, of a site of the percolation cluster. (○) $y_{CO} = 0.125$; (△) $y_{CO} = 0.50$; (■) $y_{CO} = 0.75$. The lines have been drawn to guide the eyes.

different from that seen in the classical ZGB diagram.[24] The snapshots of Figures 3b and 3c, on the other hand, provide a view of the evolution of the steady state process over the IPC and $y_{CO} = 0.8125$ for 100 and 500 million Monte Carlo Steps (MCS) (Appendix). The differences between the last two snapshots can be seen, indicating the permanent change undergone by the superficial phase as the kinetic phenomenon takes place.

As determined by Casties et al.[22] for the ZGB model, in this case the value of y_{CO}, corresponding to the phase transition y_2 at high CO concentrations, decreases linearly with the value of the blocking fraction r of the surface from $y_2 = 0.525$ on a uniform surface to approximately 0.42 in the IPC fractal. This can be explained because adsorption of O_2 requires the existence of two nearest neighbor (nn) sites on the surface. Therefore, in less branched substrates corresponding to lower values of r there is a greater number of oxygen atoms and the reaction rate is enhanced, leading to a larger value of y_2. However, the influence of the cluster's topology on the efficiency of adsorption O_2 is not seen when only one site is needed for adsorption, as in the case of CO and NO particles.

The above can explain why in our case the value of r does not have an important influence on the values of y_2 corresponding to the phase transitions of the CO–NO reaction, as seen in Figure 1 for $r \leq 0.3$, for values of $r \geq 0.3$, up to the IPC a difference is seen in the system's behavior, with loss of the approximate discontinuity of the production curves in the time range reported in this paper. This difference is also made evident by the longer time needed to achieve surface poisoning at the corresponding pressure in each case.

It has also been established by different authors that in the case of the ZGB model on random and deterministic fractals,[25,26] an IPT change from first to second-order takes place that also belongs to the universality class of directed percolation (DP). This situation has been studied in detail by Albano[26] in the case of the IPC. Figure 1 shows that apparently there is a similar situation in the CO–NO reaction if the curves for the uniform surface and the IPC fractal are compared. However, it is interesting that the discontinuity is approximately maintained in the rest of the percolation clusters, in contrast with what was found by Casties et al.[22] for the ZGB model. We have confirmed this situation, within reasonable computation times for this work, finding that for example the points on the curves corresponding to the IPC and to $r = 0.35$, for $y_{CO} > 0.8$ did not change until times as long as 500 million MCS.

Although an a priori theoretical demonstration of the character of a transition is not possible except through a mathematical experiment like the MC simulation made in this paper, in a previous paper,[27] and using as an example the ZGB model for the oxidation of CO, we proposed an explanation of the phenomenon by assuming that a heterogeneous surface can be conceived as a set of homogeneous sectors like a series of strips, for example. The argument considered that if in each of them a first-order discontinuous transition occurs at different y_{CO}, the overall result on the heterogeneous surface will be a second-order continuous transition. An argument similar to that of the ZGB model would explain the interesting character change of the transition seen in Figure 1 for the CO–NO reaction on the percolation clusters having $r > 0.3$ up to the IPC fractal.

In general, Figure 1 shows an increase of the production curves with y_{CO} for low r values, but they decrease for r values between 0.25 and the IPC. On the other hand, when the concentration of CO decreases, the curves gradually approach one another, tending to a production value close to 40 for all values of r at y_{CO} approximately equal to 0.04.

An interesting aspect is the relation found between the production values and the mean value q_i of the nearest neighbors (nn) of the active site, which caracterizes the series of percolation clusters. Figure 4 shows the activity versus q_i diagrams for different concentrations, y_{CO}, of the gas phase. q_i versus the value of r, have been determined on the computer considering the average over various substrates with the same proportion of blocked sites r.

The perfect linearity of the production versus q_i curve, with a correlation better than 0.999 in the high CO concentration zone, corresponding approximately to the maximum of the production curve, is suggestive and is mentioned below. This linearity is lost for lower y_{CO} values.

In relation to this point, it is necessary to consider that the NO dissociation stage in the mechanism of Scheme 1 is very important in the development and control of the reaction. For low y_{CO} values, the pressure of NO in the gas phase and the surface coverage θ_{NO} seen in Figure 2b are high, providing a sufficient availability of superficial nitrogen and oxygen atoms for the process. This results in a production that is almost independent of the number of neighbors of the active site, as seen in the curve of Figure 4 for $y_{CO} = 0.125$. At the other end, on the other hand, the low pressure of NO in the gas phase and the low superficial NO coverage lead to the control exerted by the number of nn of the site on the process, accounting for the proportionality found between production and q_i in the straight line of Figure 4 for $y_{CO} = 0.75$. The intermediate situation curve is shown for $y_{CO} = 0.50$.

The importance of the dissociation stage in the control of the process can also be visualized in the production curves obtained when the dissociation constant k_5 is changed. This is shown in the top insert of Figure 1 for the case of the IPC. An important decrease of the reactive window is seen

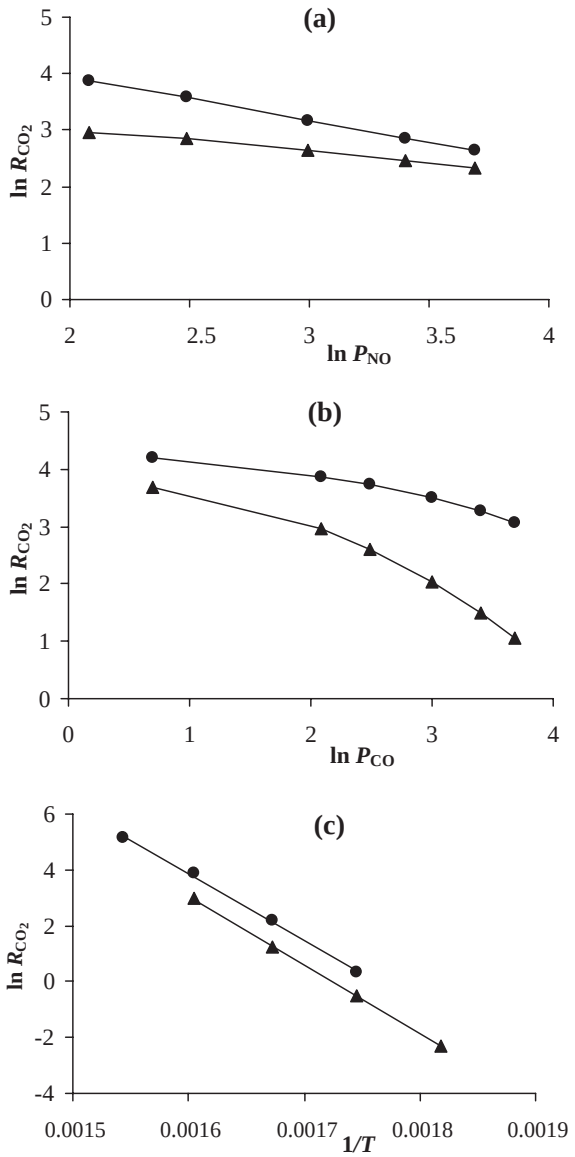

Figure 5. (a) Production R_{CO_2} as a function of NO pressure with a fixed CO pressure, $P_{CO} = 8$ Torr at 623 K; (b) R_{CO_2} production as a function of CO pressure with a fixed NO pressure, $P_{NO} = 8$ Torr at 623 K; (c) Arrhenius-like expression for $P_{CO} = P_{NO} = 8$ (Torr). The lines have been drawn to guide the eyes. (●) uniform surface; (▲) IPC.

when k_5 is increased. This is accounted for by the greater availability of nitrogen and oxygen atoms produced by the increased dissociation.

In Figure 5 we have analyzed the activity changes with the partial pressure of the system's components and with temperature, in the extremes cases of the uniform substrate and the IPC fractal within the ranges studied in this work. These relations are commonly used to determine the kinetics parameters reaction order and apparent activation energy. Figure 5a shows good linearity with a correlation better than 0.99 in the logarithmic curve of activity versus NO pressure if CO pressure is kept constant, pointing to the existence of an order with respect to NO pressure equal to -0.77 in the uniform substrate and -0.40 in the IPC. On the other hand, Figure 5b indicates that there is no reaction order in the ranges studied in the case in which P_{CO} is varied while keeping P_{NO} constant.

Figure 5c shows an adequate Arrhenius behavior of both substrates in the temperature range considered, allowing activation energies of the order of 201 kJ mol^{-1} for both surfaces, which are of the order of the experimental data, although somewhat larger than those obtained by Peden et al.,[10] for example, for the CO–NO reaction on Rh crystals. This is reasonable if one considers the approximations that belong to an MC simulation, such as the effects of the shape and size of the lattice, the non inclusion of superficial diffusion, which in this case is not considered because of the mechanism used, or the effect of having to average a large number of configurations to obtain adequate steady state values in the MC. The other factor that makes difficult the comparison with the experimental data, as we have commented previously,[19] is the uncertainty of the magnitudes of the kinetic parameters, which in general are determined in experiments under various conditions or considering mechanisms different from the one proposed recently by our group and was used in this work.

Conclusion

1) The structural sensitivity of the CO–NO reaction, manifested especially in the production diagram on the different percolation clusters from the uniform surface to the IPC fractal with the new kinetic mechanism, validates the effect of the catalysts' particle size in the actual experiment.

2) The reaction studied shows a discontinuous or first-order kinetics phase transition on the uniform surface between an active phase and one poisoned with nitrogen and oxygen, showing a degeneration that distinguishes it from that seen in the ZGB model. This discontinuity also occurs apparently in the percolation clusters only with $r \leq 0.30$, showing a clear difference in the case of the IPC. This phenomenon is different from that found by Castie for the ZGB model.

3) In the active zone, at relatively high CO pressures a perfect linearity is seen between production and the mean value of the number of nearest neighbors of the active site q_i in the cluster. In the zone of low relative CO pressures, on the other hand, there is a lower dependence of production on q_i.

4) The relation between production and pressure shows for the uniform surface and for the IPC a reasonable reaction order with respect to the NO pressure. However, no reaction order is seen in the case of CO pressure.

5) The relation between production and temperature shows an Arrhenius type behavior for the uniform surface and for the IPC, with an apparent activation energy of the order of the experimental value and slightly higher than that found by Peden et al. on single crystals of Rh. The difference has been commented in the discussion.

The authors acknowledge the financial support of this work by FONDECYT under Project No. 1070351.

Appendix

Simulation Procedure. The MC algorithm used in this paper is similar to one used previously by our group[28] for the CO oxidation reaction, based on one proposed earlier for this system[29] and recently for the CO–NO reaction.[30] For every iteration of the CO–

NO reaction, the simulation process selects an event from the mechanism (adsorption, desorption, and dissociation or surface reaction) of Scheme 1 according to the probability, p_i, of the event, defined by

$$p_i = k_i \Big/ \sum_i k_i \tag{A1}$$

where k_i corresponds to the rate constant of step i of the mechanism. It is assumed that the rate constants k_i can be expressed as functions of temperature T according to Arrhenius' equation,

$$k_i = \nu_i \exp(-E_i/RT) \tag{A2}$$

where E_i is the activation energy and ν_i is the frequency factor. In the case of adsorption, k_i is calculated according to the expression of the kinetic theory of gases:

$$k_i(\text{ads}) = \sigma(2\pi M_i RT)^{-1/2} \tag{A3}$$

where M_i is the molecular mass of i and the coefficient σ is the area occupied by 1 mol of superficial metal atoms (3.75×10^8 $\text{cm}^2\,\text{mol}^{-1}$ for Rh(111)).

Once an event has been selected, if it corresponds to the adsorption of CO, a site is chosen randomly on the surface, and if it is vacant a $CO_{(a)}$ particle will be adsorbed. If the site is occupied, the attempt is ended. If the adsorption of NO is chosen, the procedure is completely analogous, and an $NO_{(a)}$ particle is adsorbed.

If CO desorption is chosen, a surface site is selected randomly. If it is occupied by a particle other than $CO_{(a)}$ or it is vacant, the attempt is ended. However, if it is occupied by a $CO_{(a)}$ particle, desorption occurs and the particle is replaced by a vacant site. The procedure is analogous in the case of choosing the desorption of NO.

When the selected event is the dissociation of NO, a surface site is chosen randomly. If it is occupied by an $NO_{(a)}$ particle, a nearest neighbor (nn) site is chosen randomly next to the first site. If this is empty, dissociation occurs and an $N_{(a)}$ particle remains in the first site and an $O_{(a)}$ particle in the second site.

In the case of selecting a chemical reaction event, the procedure is the following: A site on the surface is first chosen randomly. In the case of the reaction between $CO_{(a)}$ and $O_{(a)}$, if the site is occupied by CO, an nn site is then chosen randomly next to the first site. If the latter is occupied by $O_{(a)}$, the event is successful and a CO_2 molecule is removed from the surface, leaving two vacant sites. If the N_2(g) production event is chosen and the first particle is $NO_{(a)}$ and the second is $N_{(a)}$, a molecule of $N_{2(g)}$ leaves the surface, leaving $O_{(a)}$ in the first site. If the selected event is N_2O production, the procedure is the same, and in this case the N_2O molecule is removed from the surface, leaving two vacant sites.

The activation energies were recalculated after every MCS, since they depend on surface coverage.

The substrates used in the simulations were a surface made of sites located in an $L \times L$ square lattice whose active sites were generated by blocking a fraction r of the $L \times L$ sites (impurities) of the square lattice. The substrates are obtained in this case by considering only the spanning cluster of the remaining sites computed by Kopelman's algorithm.[31] The case of $r = 0.407254$ corresponds to a statistical fractal, the incipient percolation cluster (IPC), with a fractal dimension equal to 91/48.[32] To achieve statistical precision it was necessary to generate a number of them, so that the properties obtained from MC for the CO–NO reaction are the average of the results of the simulations carried out on those substrates.

The lattice of $L \times L$ sites used in the simulation, with dimensions such that they contain approximately 4200 active sites for any value of r, is representative of the catalytic surface of the experiment if it is considered that the active sites of the lattice correspond to Rh atoms. In this case use has been made, as is customary for simplicity, of a square lattice with coordination equal to 4. In the case of Rh the most frequent faces are Rh(100), which is square, and Rh(111), which is hexagonal, and according to Anderson[33] the average number of atoms on the polycrystalline surface of Rh is 1.33×10^{19} ($\text{atoms}\,\text{m}^{-2}$). This means that in the simulated lattice the sites are assumed to have a separation of 0.27 nm, making it possible to relate the $L \times L$ lattice, statistically representative of the surface according to the basis of the Monte Carlo method, with the surface of the actual crystal.

In general, to reach an adequate stability in the results, use was made of a number of iterations of the order of 20 million Monte Carlo Steps (MCS), defined as a number of attempts equal to the number of sites in the substrate. This stability was checked in several cases, verifying that the result did not vary at all after 500 million MCS.

References

1 G. Nicolis, I. Prigogine, *Self-Organization in Nonequilibrium Systems*, Wiley Interscience, New York, **1977**; H. Haken, *Synergetics*, Springer-Verlag, New York, **1977**; J. Marro, R. Dickman, *Nonequilibrium Phase Transitions in Lattice Models*, University Press, Cambridge, **1999**.

2 K. C. Taylor, *Catal. Rev.—Sci. Eng.* **1993**, *35*, 457; M. Shelef, G. Graham, *Catal. Rev.—Sci. Eng.* **1994**, *36*, 433.

3 J. W. Evans, *Langmuir* **1991**, *7*, 2514.

4 V. P. Zhdanov, B. Kasemo, *Surf. Sci. Rep.* **1994**, *20*, 111.

5 E. V. Albano, *Heterog. Chem. Rev.* **1996**, *3*, 389; E. V. Albano, M. Borowko, *Computational Methods in Surface and Colloid Science*, Marcel Dekker, New York, **2000**, Chap. 8, pp. 387–437.

6 W. C. Hecker, A. T. Bell, *J. Catal.* **1983**, *84*, 200.

7 S. H. Oh, G. B. Fisher, J. E. Carpenter, D. Wayne Goodman, *J. Catal.* **1986**, *100*, 360.

8 B. K. Cho, *J. Catal.* **1992**, *138*, 255; **1994**, *148*, 697.

9 H. Permana, Ng. K. Simon, Ch. Peden, S. J. Schmieg, D. K. Lambert, D. N. Belton, *J. Catal.* **1996**, *164*, 194.

10 C. H. F. Peden, D. N. Belton, S. J. Schmieg, *J. Catal.* **1995**, *155*, 204.

11 S. Chuang, C. Tan, *J. Catal.* **1998**, *173*, 95.

12 F. Zaera, S. Wehner, C. S. Gopinath, J. L. Sales, V. Gargiulo, G. Zgrablich, *J. Phys. Chem. B* **2001**, *105*, 7771.

13 C. S. Gopinath, F. Zaera, *J. Catal.* **1999**, *186*, 387; F. Zaera, C. S. Gopinath, *J. Chem. Phys.* **1999**, *111*, 8088.

14 J. Cortés, E. Valencia, *J. Phys. Chem. B* **2006**, *110*, 7887.

15 K. Yaldram, M. A. Khan, *J. Catal.* **1991**, *131*, 369.

16 B. Meng, W. H. Weinberg, J. W. Evans, *Phys. Rev. E* **1993**, *48*, 3577.

17 B. J. Brosilow, R. M. Ziff, *J. Catal.* **1992**, *136*, 275.

18 J. Cortés, E. Valencia, *Phys. Rev. E* **2005**, *71*, 46136.

19 J. Cortés, E. Valencia, *J. Phys. Chem. B* **2004**, *108*, 2979; J. Cortés, E. Valencia, J. Herrera, P. Araya, *J. Phys. Chem. C* **2007**, *111*, 7063.

20 J. Cortés, H. Puschmann, E. Valencia, *J. Chem. Phys.* **1996**, *105*, 6026; J. Cortés, H. Puschmann, E. Valencia, *J. Chem. Phys.* **1998**, *109*, 6086.

21 A. G. Dickman, B. C. Grandi, W. Figueiredo, R. Dickman,

Phys. Rev. E **1999**, *59*, 6361.
22 A. Casties, J. Mai, W. von Niessen, *J. Chem. Phys.* **1993**, *99*, 3082.
23 D. N. Belton, C. L. DiMaggio, S. J. Schmieg, K. Y. S. Ng, *J. Catal.* **1995**, *157*, 559.
24 R. M. Ziff, E. Gulari, Y. Barshad, *Phys. Rev. Lett.* **1986**, *56*, 2553.
25 J. Mai, A. Casties, W. von Niessen, *Chem. Phys. Lett.* **1992**, *196*, 358; A. Y. Tretyakov, H. Takayasu, *Phys. Rev. A* **1991**, *44*, 8388.
26 E. V. Albano, *Phys. Rev. B* **1990**, *42*, 10818.
27 J. Cortés, E. Valencia, *Surf. Sci.* **1999**, *425*, L357.
28 J. Cortés, E. Valencia, P. Araya, *J. Chem. Phys.* **1998**, *109*, 5607.
29 P. Araya, W. Porod, E. E. Wolf, *Surf. Sci.* **1990**, *230*, 245; P. Araya, W. Porod, R. Sant, E. E. Wolf, *Surf. Sci.* **1989**, *180*, 208.
30 L. Olsson, V. P. Zhdanov, B. Kasemo, *Surf. Sci.* **2003**, *529*, 338.
31 J. Hoshen, R. Kopelman, *Phys. Rev. B* **1976**, *14*, 3438; R. Kopelman, *J. Stat. Phys.* **1986**, *42*, 185.
32 D. Stauffer, A. Akarony, *Introduction to Percolation Theory*, 2nd ed., Taylor and Francia, London, **1992**.
33 J. R. Anderson, *Structure of Metallic Catalysts*, Academic Press, London, New York, San Francisco, **1975**.